Channel Formation by Salmon and Human Calcitonin in Black Lipid Membranes

Valentina Stipani,* Enrico Gallucci,* Silvia Micelli,* Vittorio Picciarelli,† and Roland Benz‡
*Dept. Farmaco-Biologico, †Dept. Interateneo di Fisica, Università degli Studi di Bari, I-70126 Bari, Italy, and ‡Lehrstuhl für Biotechnologie, Theodor-Boveri-Institut (Biozentrum) der Universität Würzburg, Am Hubland, D-97074 Würzburg, Germany

ABSTRACT In this study we investigated the interaction of salmon and human calcitonin (Ct) with artificial lipid bilayer membranes. Both peptides were able to form either transient or permanent channels in the model membranes. The channels formed by salmon Ct at concentration (125 nM) had, on average, a single-channel conductance of 0.58 ± 0.04 nS in 1M KCl (+10 mV), which is voltage-dependent at lower voltages. Human Ct forms at the same concentration channels with a much lower probability, and high voltages of up to +150 mV were needed to initiate channel formation. The estimated single-channel conductance formed under these conditions was ~0.0119 ± 0.0003 nS in 1 M KCl. Both salmon and human Ct channels were found to be permeable to calcium ions. The possibility is discussed that the superior therapeutic effect of salmon Ct as a tool to treat bone disorders, including Paget disease, osteoporosis, and hypercalcemia of malignancy, rather than human Ct is related to the lack of the fibrillating property of salmon Ct. Preliminary data indicate that also eel and porcine Ct and carbocalcitonin form channels in model membranes.

INTRODUCTION

Calcitonin (Ct), a small peptide hormone, is present in all vertebrates. Its structure is consistent with an N-terminal portion, considered specific for receptor activation, and a helical segment in the central part of the molecule that is more variable in contrast to the highly conserved C- and N-termini (Sexton et al., 1999). Ct has an important effect on Ca^{2+} metabolism because it inhibits osteoclast-mediated bone resorption and induces calcium uptake from body fluids. This hypocalcemic response is caused by an inhibitory action of Ct on osteoclast resorption. This action is responsible for its widespread clinical use for the treatment of bone disorders, including Paget disease and hypercalcemia of malignancy (Wallach et al., 1999). Ct is considered an inhibitor of bone resorption and an important tool against osteoporosis. Furthermore, salmon calcitonin (sCt), but not human calcitonin (hCt), prevents or retards bone loss and increases bone strength in rat and other species. A similar anabolic effect is also found for cartilage formation, bone matrix synthetic activity, and bone growth (Wallach et al., 1999). New approaches to prevent osteoporosis and to regenerate cartilage have been developed using novel Ct-like molecules (Torres-Lugo and Peppas, 2000). Moreover, other biological activities have been recognized, such as its action on the thick ascending limb of the loop of Henle and its role as a neurotransmitter or neuromodulator in the nervous system (Fisher et al., 1981). A neurotrophic effect of sCt on serotonergic neurons has also been found (Boujard et al., 1998). Most of these actions are mediated through a superfamily of 7 trans-membrane-spanning helices G protein-coupled receptors that act via a second messenger, adenylyl cyclase and/or the phosphoinositide-specific phospholipase C pathways (Segre and Goldring, 1993). The secondary structure of Ct has been studied in different environments using various spectroscopic techniques (Epand et al., 1983; Motta et al., 1991; Arvinte and Drake, 1993; Siligardi et al., 1994; Hashimoto et al., 1999). Fluorescence, circular dichroism (CD), and infrared spectroscopy suggest that sCt and hCt adopt an α-helical structure comprising up to 40–48% of the amino acids in methanol/water and trifluoroethanol/water mixtures. sCt adopts the α-helical structure more readily than hCt when solvent polarity is reduced (Arvinte and Drake, 1993). This may be linked with the longer lifetime of sCt as compared with hCt in vivo (Epand et al., 1983). CD measurements demonstrate that hCt adopts β-sheet conformation when it interacts with neutral and negatively charged liposomes (Schmidt et al., 1998). Ct seems to react strongly with negatively charged lipids such as phosphatidylglycerol and phosphatidic acid, whereas only moderate or no interaction is observed with several other phospholipids (Epand et al., 1983). Comparative studies of hCt and sCt secondary structure in solutions with low dielectric constants shows a shorter helix length and no-helix tail interaction for hCt, whereas the structure of sCt contains flexible loops connecting the head and the helix, and the helix and the tail region (Amodeo et al., 1999). The topologies of Cts associated with oriented lipid bilayers were also determined with solid-state NMR. In agreement with CD measurement the peptides have an identical conformation in micelles, which is characterized by an amphipathic α-helix consisting of residues Ser^5 through Leu^{19} followed by an unstructured region at the C-terminus (Hashimoto et al., 1999). A similar structure has been observed in sodium dodecyl sulfate micelles, which suggests that the main conformational feature of the peptide

Received for publication 26 February 2001 and in final form 17 August 2001.

Address reprint requests to Silvia Micelli, Dipartimento Farmaco-Biologico, Università degli Studi di Bari, I-70126 Bari, Italy. Tel.: 39-080-5442775; Fax: 39-080-5442796; E-mail: micelli@farmbiol.uniba.it

0006-3495/01/12/3332/07 $2.00

hormone is an α-helix from Thr^{6} through Tyr^{22}, thus including the amphipathic 8–22 segment and two residues of the Cys1-Cys7 N-terminal loop (Motta et al., 1991).

Neutron diffraction of oriented multilayers has also been used to study the interaction of the amphipathic peptide sCt with different lipids. Important for the study of the interaction is the addition of 15% (mol) of the anionic phospholipid 1,2-dioleoyl-*sn*-glycero-phosphoglycerol (DOPG) to 1,2-dioleoyl-*sn*-glycero-phosphocholine (DOPC). Neutron-scattering profiles show a continuous band of deuterons across each bilayer, which suggests that the hormone forms transbilayer α-helixes similar to certain peptides such as alamethicin (Tosteson et al., 1990) and melittin (Hall et al., 1984). These experiments suggest a possible evolutionary history for Ct, and that sCt may have ion-channel activity (Bradshaw, 1997).

The planar lipid bilayer system provides an elegant way to study membrane-active compounds. We used electrophysiological methods to investigate the characteristics of the incorporation of sCt and hCt into model black lipid bilayer membranes (BLM) and their dependence on the applied voltage. The results suggest that both sCt and hCt show channel-forming activity in lipid bilayer membranes but at different concentrations, which is probably related to the peculiar fibrillation property of hCt.

MATERIALS AND METHODS

Planar membrane experiments

Two different techniques were used to study the interaction of the Cts with BLM: alternating current measurements (AC method) and single-channel measurements. In both cases, Teflon (DuPont, Wilmington, DE) chambers were used that had two aqueous compartments connected by small circular holes. The holes' diameter was 1.3 mm for the AC method or 0.3 mm for the single-channel experiments. BLM were formed across the holes as has been described (Benz et al., 1978). Membranes were formed with a 1% (w/v) solution of a mixture of DOPC and DOPG (molar ratio 85:15) in *n*-decane or from pure DOPC dissolved in *n*-decane. The salts used in the experiments were of analytical grade. The aqueous solutions were used unbuffered and had a pH of 7.

The AC method has been described in detail elsewhere (Gallucci et al., 1996; Micelli et al., 2000). A generator mixing 1 Hz of variable amplitude (V_s) and 1 KHz of 2 mV signals applied the voltage to a platinum electrode situated in one compartment of the cell. The output voltage, acquired through a second platinum electrode in the other compartment, was electronically amplified and filtered to separate the two frequency components. The data were collected via a PC computer interfaced with two voltage-frequency converters and stored on floppy disk for further analysis (Vernier software, http://www.vernier.com).

In single-channel experiments, membrane current was measured either with a pair of Ag/AgCl electrodes with salt bridges switched in series with a voltage source and a high sensitive current amplifier (Keithley 427) or with a pair of Ag/AgCl electrodes in ion selectivity experiments.

The amplified signal was monitored with a storage oscilloscope and recorded with a tape recorder or a strip chart recorder. The single-channel instrumentation had a time resolution of 1–10 msec depending on the magnitude of the single-channel conductance. The polarity of the voltage was defined with respect to the side where the Ct was added (the *cis*-side). A *trans*-negative potential (indicated by a minus sign) means that a negative potential was applied to the *trans*-side, the compartment opposite to the one where Ct was added. In some experiments, Ct was added to both aqueous phases of BLM without affecting the results. Perfusion was performed by simultaneously withdrawing the bathing media and adding fresh fluid. The single-channel data were obtained from at least 2–4 experiments performed on different days. All single-channel events (>100 single channel events for each experiments) were used to calculate the event amplitudes, irrespective of duration. An histogram of amplitude distribution for each experiment was constructed and fitted by a Gaussian distribution function (GraphPad Prism version 3.0; GraphPad Software, http://www.graphpad.com). Results are expressed as mean ± SE.

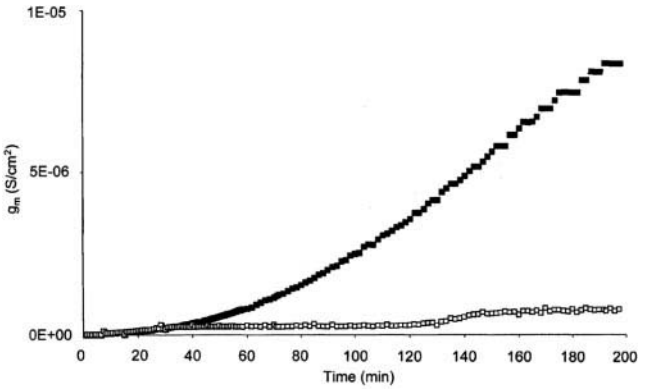

FIGURE 1 Time course of membrane conductance. Time course of membrane conductance, g_m (Siemens/cm^2) of a lipid bilayer membrane made from DOPC/DOPG after addition at zero time of 85 nM sCt (■) and time course of undoped membrane conductance (□). The aqueous phase contained 1 M KCl, pH 7. The temperature was 20°C; $R_l = 1$ MΩ; $C_l = 20$ nF; $f = 0.5$ Hz; $V_s = 80$ mV. The starting conductance of BLM was $1.5 \cdot 10^{-8}$ S/cm^2.

Chemicals

Salts and other basic chemicals were bought from Merck (analytical grade, Darmstadt, Germany) and biochemicals from Sigma (Munich, Germany). The phospholipids used in this study were purchased from Avanti Polar Lipids (Alabaster, AL). sCt and hCt were kind gifts from Novartis Pharma AG (Basel, Switzerland); porcine and eel Ct were purchased from Calbiochem (San Diego, CA); and carbocalcitonin was purchased from Smithkline Beecham (Okayama, Japan).

RESULTS

Macroscopic conductance measurements

In a first set of experimental conditions we studied the effect of sCt on the conductance of lipid bilayer membranes using the AC method. After addition of 85 nM sCt to DOPC/DOPG, the specific conductance increased on average from $4.7 \cdot 10^{-7} \pm 8.4 \cdot 10^{-8}$ S/cm^2 to $1.53 \cdot 10^{-5} \pm 3.24 \cdot 10^{-6}$ S/cm^2 (average ± SE of four experiments). Fig. 1 shows a representative experiment of the specific conductance increase of membrane after addition of sCt to the aqueous phase, as compared with undoped membrane. It is noteworthy, however, that the membranes were found to be fairly stable under these conditions (85 nM) (Fig. 1). Higher sCT

TABLE 1 The effective conductance of Cts

Calcitonin	$\Lambda \pm$ SE (nS)	n. exp.
Eel	0.042 ± 0.0014	2
Porcine	0.056 ± 0.005	2
Salmon	0.09 ± 0.007	7
Carbocalcitonin	0.042 ± 0.0006	2

Average single-channel conductance Λ of the Cts (125 nM) for 1M KCl solution, at +50 mV voltages. The membranes were formed from DOPC/DOPG. The aqueous solutions were at pH 7; T = 20°C.

concentrations tended to reduce membrane stability (data not shown). It is possible that the instability of the membrane at higher sCt concentrations reflected some sort of detergent effect mediated by the peptide. The effect of hCt on membranes made from the same lipids was less reproducible than that shown for sCt. However, a higher reproducibility was obtained at lower hCt concentration (24.5 nM), where the conductance also increased approximately two orders of magnitude within 200 min (data not shown).

It is possible that the conductance increase described above was caused by an unspecific artifact. To rule that possibility out, we performed control experiments where trypsin was added to the aqueous phase before the addition of Ct. Under these conditions we observed only an insignificant increase in membrane-specific conductance of approximately a factor of two within 200 min. Similarly, we found also an insignificant effect on membrane-specific conductance when the hormones were pretreated with trypsin before they were added to the salt solution on one or both sides of the membrane. These results indicated that the conductance increase reported in Fig. 1 and similar experiments was caused by Ct and did not represent an artifact.

Single-channel recording

To study the interaction between Ct and BLM in more detail, we performed single-channel conductance measurements. These experiments are considered a sensitive tool for the study of channel-forming substances. For these measurements, it is important that the substances form defined channels and do not act as detergents inducing lipid perturbation. The observation of nonrandom discrete step-like increases in conductance could be considered to conform to these criteria. Preliminary experiments indicate that all Cts tested (eel, porcine, carbocalcitonin, human, and salmon) when added to one or both sides of the BLM kept under voltage-clamp conditions are able to form channels (Table 1). In this study, we focused our attention on two Cts, namely sCt and hCt. Shortly after the addition of Cts, we observed a stepwise increase in membrane conductance, which indicated the formation of ion-permeable channels in the membranes. Fig. 2 shows a single-channel recording with associated histogram of channel conductance distribution derived from such an experiment with sCt (125 nM), in

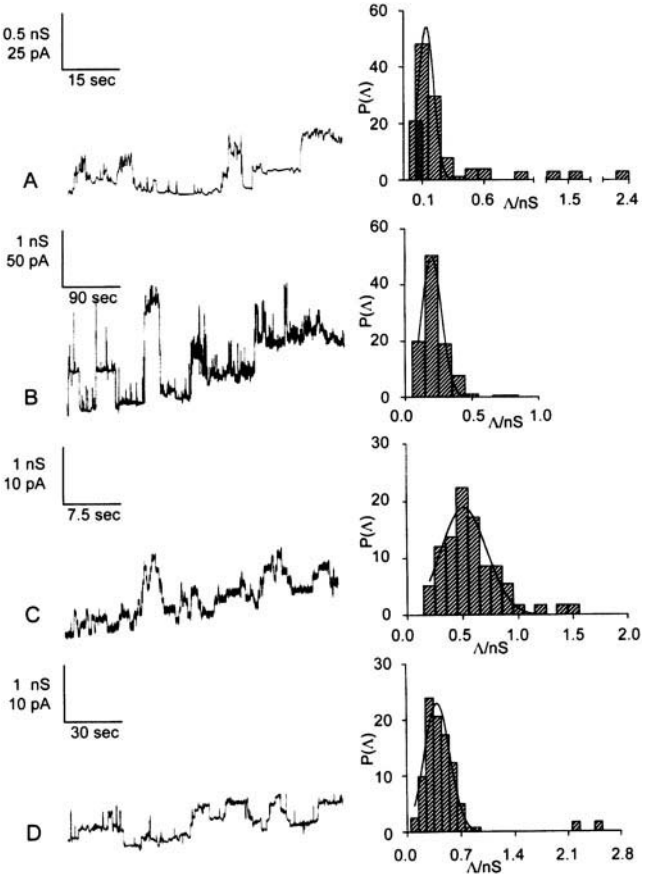

FIGURE 2 Chart recorder tracing with associated distribution histogram of sCt channel conductance events. Experiments on DOPC/DOPG (molar ratio 85:15) membrane in the presence of 125 nM sCt added to both sides. T = 20°C. (*A*) The voltage was set to +50 mV and the aqueous phase contained 1 M KCl (pH 7), 76_{mean} = 0.133 ± 0.005 nS (166 events). (*B*) The voltage was set to +50 mV and the aqueous phase contained 1 M NaCl (pH 7), 76_{mean} = 0.2 ± 0.006 nS (194 events). (*C*) The voltage was +10 mV and the aqueous phase contained 1 M KCl (pH 7), 76_{mean} = 0.51 ± 0.02 nS (200 events). (*D*) The voltage was +10 mV and the aqueous phase contained 0.3 M KCl (pH 7), 76_{mean} = 0.4 ± 0.014 nS (194 events). Each recording represents a fragment of the recording obtained in an independent experiment. Histogram of the probability *P*(76) for the occurrence of a given conductivity unit. Gaussian fit is shown as a solid curve.

which different applied voltages and/or different bathing media were used. The single-channel recordings shown in Fig. 2 demonstrate that discrete conductance steps were observed in the presence of sCt. The conductance fluctuations were not uniform in size and most of the steps were directed upwards, whereas downward steps (closing channel) were more rarely observed under these conditions. Fig. 3 shows examples of single-channel recording with associated histograms of the distribution of sCt and hCt channel conductance for membranes bathed in 1 M KCl. The current fluctuations were distributed over a conductance range of 0.0066–0.125 nS for sCt (125 nM, +150 mV) (Fig. 3 *A*) and over a range of 0.02–0.12 nS for sCt (49 nM, +50 mV) (Fig. 3 *B*). The mean value of single-channel conductance

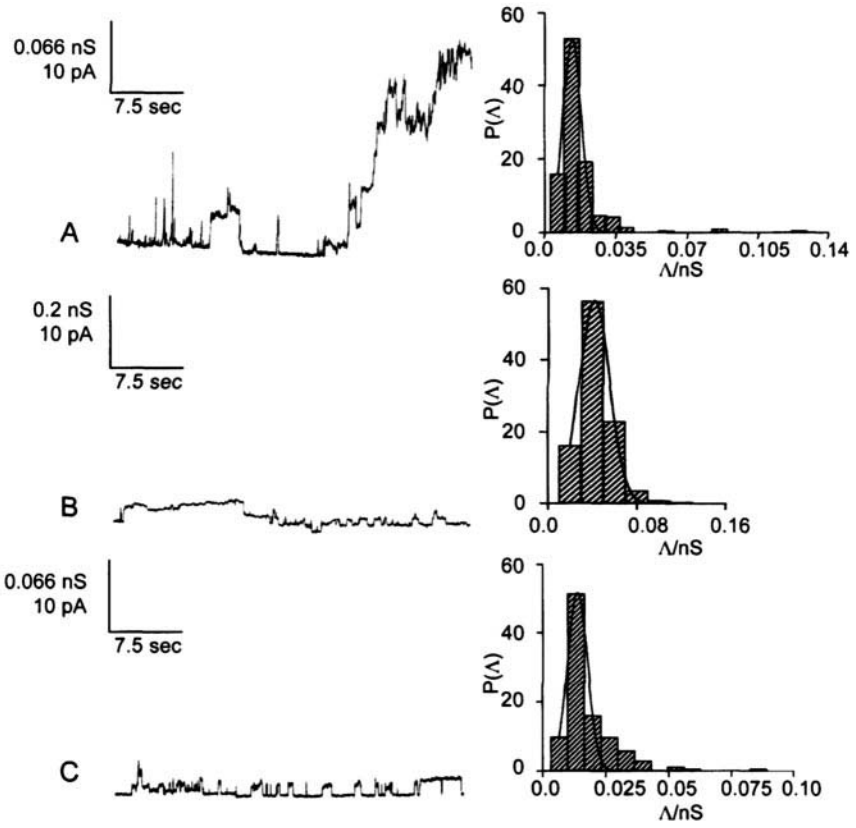

FIGURE 3 Chart recorder tracing with associated histogram of the conductance fluctuations of sCt and hCt. Single-channel recording of membranes formed of DOPC/DOPG (molar ratio 85:15) membranes. The aqueous phase contained 1 M KCl, pH 7, and sCt or hCt in a concentration of 125 nM (*A*, *C*) and 49 nM (*B*) on both sides of the membrane; T = 20°C. (*A*) The average single-channel conductance of 253 single-channel events was 0.0135 ± 0.0003 nS at +150 mV. (*B*) The average single-channel conductance of 236 single-channel events was 0.04 ± 0.0005 nS at +50 mV. (*C*) The average single-channel conductance of 175 single-channel events was 0.0138 ± 0.0005 nS at +150 mV. Histogram of the probability *P*(76) for the occurrence of a given conductivity unit. Gaussian fit is shown as a solid curve.

for sCt at concentration of 125 nM (+150 mV) and 49 nM (+50 mV) was 0.0135 ± 0.0003 nS and 0.042 ± 0.0005 nS, respectively.

At +50 mV it was not possible to observe channels in membranes when hCt was present in a concentration of 125 nM. Interestingly, channel-forming activity of hCt increased when the voltage across the membrane was increased. The current fluctuations were distributed over a conductance range of 0.0066–0.085 nS (125 nM, +150 mV)(Fig. 3 *C*). The average single-channel conductance for hCt was 0.0138 ± 0.0005 nS (+150 mV). It is noteworthy that we observed a similarly broad distribution of the single-channel conductance in experiments where the membranes were bathed in 1 M NaCl, 1 M $CaCl_2$, and 1 M KCH_3COO (data not shown). Table 2 summarizes the single-channel conductance data of sCt obtained with DOPC/DOPG membranes bathed in different salt solutions. The results of Table 2 suggest that considerable variations to the single-channel conductances were observed under different conditions. One interesting result is that the single-channel conductance decreased as a function of the applied voltage (Fig. 4). The preliminary investigation was performed by running the experiment at different voltages or by changing the applied potential during the experiment (data not reported). The hCt channel showed the same pattern (data not shown). It is noteworthy that many other small peptides that form α-helical structures in lipid membranes such as mellitin (Tosteson et al., 1990), gramicidin A (Bamberg et al., 1977), or alamethicin (Hall et al., 1984) tend to show increased chan-

TABLE 2 The effective conductance of sCt for different salt solutions

Ion	Λ ± SE (nS)	n. exp.
1 M NaCl	0.19 ± 0.006	2
1 M $CaCl_2$	0.22 ± 0.0064	2
1 M KCH_3COO	0.23 ± 0.016	2
1 M KCl	0.09 ± 0.007	7

Average single-channel conductance Λ of the sCt (125 nM) for different salt solutions at positive voltage of +50 mV. The membranes were formed from dOPC/DOPG (molar ratio 85:15). The aqueous solutions were at pH 7; T = 20°C.

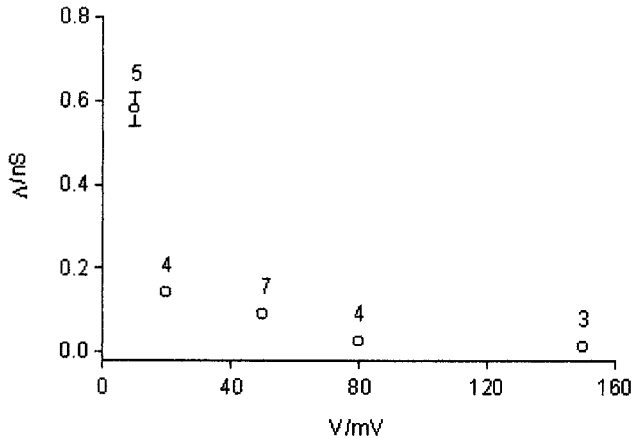

FIGURE 4 Conductance of sCt versus different membrane potential. Average single-channel conductance 76 of the sCt (125 nM) as function of applied voltage. The membranes were formed from DOPC/DOPG (molar ratio 85:15). The aqueous solutions were at pH 7; T = 20°C.

nel size and increased channel-forming activity when the voltage increases. This probably means that sCt (and perhaps hCt as well) has no dipole moment.

Ion selectivity

The ion channel selectivity of the channels formed by sCt was investigated by measuring the membrane potential under zero current conditions. DOPC/DOPG membranes were formed in 0.3 M solution of KCl or 0.3 M NaCl. After blackening of the membranes, sCt was added in a final concentration of 125 nM to both sides. About 20 min after the addition, the membrane conductance reached a virtually stable value; then the salt concentration on one side of the membranes was raised up to 0.5 M by addition of concentrated salt solution. In all cases, the more diluted side (*trans* to salt addition) became slightly positive (+1 mV for 0.5 M at the *trans* side) indicating that channels are almost equally permeable to anions and cations. Analysis of the zero current membrane potentials using the Goldman-Hodgkin-Katz equation (Benz et al., 1979) gives a P_c/P_a of 1.03.

DISCUSSION

sCt and hCt form ion-permeable channels in lipid bilayer membranes

For the first time, this study demonstrates channel formation by Cts, in particular sCt and hCt, in BLM made of DOPC/DOPG mixtures. Moreover, preliminary experiments clearly indicate that other Cts (eel, porcine, carbocalcitonin) also form channels (Table 1). The sCt channels show a strong voltage-dependence; in fact, they had a single-channel conductance of 0.58 ± 0.04 nS at +10 mV and 0.0123 ± 0.0003 nS at +150 mV applied voltage, and showed a broad distribution of the single-channel conductance. Furthermore, we observed different lifetimes for the channels ranging from seconds to many minutes. The reason for this variability is not clear. It could be caused by the generation of multistate channels, as has been shown for other small peptides, such as alamethicin and mellitin (Tosteson et al., 1990; Hall et al., 1984), but we do not yet have a clear indication for multistate channels in the case of sCt.

The average single-channel conductance of the sCt channel followed the specific conductivity of the aqueous salt solutions. This result suggests that ions may move inside the channel as they do in the aqueous phase without much interaction with the channel wall.

It is known that amphipathic α-helix formation induced by lipids' surface is a prerequisite for membrane peptide penetration (Jacobs and White, 1989; Engelman and Steitz, 1981; Milik and Skolmick, 1993). It has been proposed that the first step could be a salt bridge between the amino acid lysine and the phosphate group of the phospholipid molecules, which acts as an "interfacial anchor " (Jacobs and White, 1989; Bechinger et al., 1999). This interaction allows the hydrophobic part of peptide molecule to contact the methylene part of lipid, followed by peptide penetration into membrane. It is worth noting that no channel activity has been found by both sCt and hCt in both DOPC and egg phosphatidylcholine (palmitoyl-oleoyl-phosphatidylcholine) membranes, a finding that corroborates the observation of Epand et al. (1983), who found that Ct did not interact with zwitterionic lipid dimyristoylphosphatidylcholine (DMPC). This result can be relevant in targeting the Ct on specific membranes. Moreover, Motta et al. (1998) have reported NMR spectra for hCt indicative of an α-helix between residues 9 and 16 with exclusion of Asn^{17}-Lys^{18}-$Phen^{19}$ regions from the helix; from His^{20} the hormone takes up an extended structure with no interaction with the helix in contrast with sCt where the C-terminal decapeptide shows apposition to the helix. This structural feature can account for the different degree of interaction with membranes, especially when relatively high concentrations of hCt are used, where the hydrophobic side of the helix can trigger intermolecular interaction culminating in the fibrillation as demonstrated by the minor channel activity at higher hCt concentration.

In this context, it has been suggested that internalization of hCt into nasal mucosa is associated with β-sheet–induced self-assembly of the C-terminal segment of the peptide (Schmidt et al., 1998). In contrast, it has been demonstrated that hCt has considerably less α-helical structure than sCt in the presence of negatively charged lipids (Epand et al., 1983), which may explain the previously reported faster rate of degradation of hCt compared with sCt in vivo. However, Gilchrist and Bradshaw (1993) have demonstrated that sCt also can form amyloid fibrils at concentrations of 10 mg/ml in vitro. This suggests that hCt may have a lower channel-

forming activity at 125 nM concentration, and a higher applied potential across the membrane can counteract this failure.

The Ct channel is probably formed by a Ct oligomer

Studies of the membrane-bound secondary structure of the Cts have revealed that they have a mostly α-helical structure (Motta et al., 1991; Hashimoto et al., 1999; Bradshaw et al., 1996; Bradshaw, 1997). However, the Cts contain only a few windings, which means that the helix of sCt is too short to span the bilayer as its α-helical structure is only 16 amino acids long, whereas ~20 amino acids are needed to span the hydrocarbon core of a membrane (Motta et al., 1991). Furthermore, the Cts contain also a β-sheet portion. This portion is essential for Ct-lipid interaction (Schmidt et al., 1998), but again, this part of the molecule is not long enough to cross a BLM. This means that the Ct must aggregate into oligomers to form a channel. This is possible because they present a high degree of conformation flexibility, depending on the chemical nature of environment.

Is channel formation related to Ct function?

hCt and sCt are routinely used as therapeutic tools because of their inhibitory action on osteoclast-mediated bone resorption. In particular, these polypeptide hormones are widely used clinically for the treatment of bone disorders, including Paget disease, osteoporosis, and hypercalcemia of malignancy (Sexton et al., 1999; Lane et al., 2000). Furthermore, other actions in which Ct have been involved concern neuromodulation and/or neurotransmission (Fisher et al., 1981).

The major therapeutic activity shown by sCt may be explained by a greater internalization of sCt and/or its longer lifetime in vivo because of the formation of a α-helical structure, which may also facilitate channel formation. Cationic peptides such as alamethicin, mellitin, and magainin are able to interact with negatively charged lipids, incorporate into the membrane, and form channels (Tosteson et al., 1990; Bamberg et al., 1977; Boheim, 1974). This causes flips of lipids (Matzuzaky et al., 1998), determining brief perturbation of the membrane. As Ct shares similar properties to the peptides cited above, at physiological concentrations the perturbation induced on the membrane may be useful to trigger signal transduction through receptor interaction. However, this effect may be magnified by the increase in permeability determined by the hormone-channel to calcium. An extra source of calcium provided by Ct channel formation at the membrane surface may add relevance to the function related with intracellular calcium homeostasis. Thus, all Cts tested here may be included in the category of small peptides having biological and pharmacological properties which are receiving particular interest because of their channel-like activity and bilayer perturbation (Sahl et al., 1987; Boheim, 1974; Bechinger et al., 1993; Grant et al., 1992; Williams et al., 1990).

We thank Novartis Pharma AG for kindly providing human and salmon calcitonin. We thank Anthony Green (green@pangeanet.it.) for proofreading the English. This work was supported by grants of the Deutsche Forschungsgemeinschaft (Sonderforschungsbereich 487, project A5) and the Fonds der Chemischen Industrie to R.B. and CNR (Italy).

REFERENCES

Amodeo, P., A. Motta, G. Strazzullo, and M. A. Castiglione Morelli. 1999. Conformational flexibility in calcitonin: the dynamic properties of human and salmon calcitonin in solution. *J. Biomol. NMR.* 13:161–174.

Arvinte, T., and A. F. Drake. 1993. Comparative study of human and salmon calcitonin secondary structure in solutions with low dielectric constants. *J. Biol. Chem.* 268:6408–6414.

Bamberg, E., H. J. Apell, and H. Alpes. 1977. Structure of the gramicidin A channel: discrimination between the piL, D and the β helix by electrical measurements with lipid bilayer membranes. *Proc. Natl. Acad. Sci. U.S.A.* 74:2402–2406.

Bechinger, B., J. M. Ruysschaert, and E. Goormaghtigh. 1999. Membrane helix orientation from linear dichroism of infrared attenuated total reflection spectra. *Biophys. J.* 76:552–563.

Bechinger, B., M. Zasloff, and S. J. Opella. 1993. Structure and orientation of the antibiotic peptide magainin in membranes by solid-state nuclear magnetic resonance spectroscopy. *Protein Sci.* 2:2077–2084.

Benz, R., K. Janko, W. Boos, and P. Läuger. 1978. Formation of large, ion-permeable channels by the matrix protein (porin) of *Escherichia coli. Biophys. J.* 511:305–319.

Benz, R., K. Janko, and P. Läuger. 1979. Ionic selectivity of pores formed by the matrix protein (porin) of *Escherichia coli. Biochim. Biophys. Acta.* 551:238–247.

Boheim, G. 1974. Statistical analysis of alamethicin channels in black lipid membranes. *J. Membrane Biol.* 19:277–303.

Boujard, F., F. Dauphin, and R. de Blaurepaire. 1998. Calcitonin increases 5-HT1A binding in the brain of adrenalectomized rats. *Brain Res.* 812:279–282.

Bradshaw, J. P. 1997. Phosphatydylglycerol promotes bilayer insertion of salmon calcitonin. *Biophys. J.* 72:2180–2186.

Bradshaw, J. P., K. C. Duff, P. J. Gilchrist, and A. M. Saxena. 1996. Neutron diffraction studies of amphipathic helices in phospholipid bilayers. *Basic Life Sci.* 64:191–202.

Engelman, D. M., and T. A. Steitz. 1981. The spontaneous insertion of proteins into and across membranes: the helical hairpin hypothesis. *Cell.* 23:411–422.

Epand, R. M., R. F. Epand, R. C. Orlowski, R. J. Schlueter, L. T. Boni, and S. W. Hui. 1983. Amphipathic helix and its relationship to the interaction of calcitonin with phospholipids. *Biochemistry.* 22:5074–5084.

Fisher, J. A., P. H. Tobler, M. Kaufmann, W. Born, H. Henke, P. E. Cooper, S. M. Sagar, and J. B. Martin. 1981. Calcitonin: regional distribution of the hormone and its binding sites in the human brain and pituitary. *Proc. Natl. Acad. Sci. U.S.A.* 78:7801–7805.

Gallucci, E., S. Micelli, and G. Monticelli. 1996. Pore formation in lipid bilayer membranes made of phosphatidylinositol and oxidized cholesterol followed by means of alternating current. *Biophys. J.* 71:824–831.

Gilchrist, P. J., and J. P. Bradshaw. 1993. Amyloid formation by salmon calcitonin. *Biochim. Biophys. Acta.* 1182:111–114.

Grant, E. Jr., T. J. Beeler, K. M. Taylor, K. Gable, and M. A. Roseman. 1992. Mechanism of magainin 2a induced permeabilization of phospholipid vesicles. *Biochemistry.* 31:9912–9918.

Hall, J. E., I. Vodyanoy, T. M. Balasubramanian, and G. R. Marshall. 1984. Alamethicin: a rich model for channel behavior. *Biophys. J.* 45:233–247.

Hashimoto, Y., K. Toma, J. Nishikido, K. Yamamoto, K. Haneda, T. Inazu, K. G. Valentine, and S. J. Opella. 1999. Effects of glycosylation on the structure and dynamics of eel calcitonin in micelles and lipid bilayers determined by nuclear magnetic resonance spectroscopy. *Biochemistry.* 38:8377–8384.

Jacobs, R. E., and S. H. White. 1989. The nature of the hydrophobic binding of small peptides at the bilayer interface: implications for the insertion of transbilayer helices. *Biochemistry.* 28:3421–3437.

Lane, J. M., L. Russell, and S. N. Khan. 2000. Osteoporosis. *Clin. Orthop.* 372:139–150.

Matzuzaky, K., Y. Mitani, K. Y. Akada, O. Murase, S. Yoneyama, M. Zasloff, and K. Miyajima. 1998. Mechanism of synergism between antimicrobial peptides magainin 2 and PLGa. *Biochemistry.* 37: 15144–15153.

Micelli, S., E. Gallucci, and V. Picciarelli. 2000. Studies of mitochondrial porin incorporation parameters and voltage-gated mechanism with different black lipid membranes. *Bioelectrochemistry.* 52:63–75.

Milik, M., and J. Skolmick. 1993. Insertion of peptide chains into lipid membranes: an off-lattice Monte Carlo dynamics model. *Proteins.* 15: 10–25.

Motta, A., G. Andreotti, P. Amodeo, G. Strazzullo, and M. A. Castiglione Morelli. 1998. Solution structure of human calcitonin in membrane-mimetic environment: the role of the amphipathic helix. *Proteins.* 32: 314–323.

Motta, A., A. Pastore, N. A. Goud, and M. A. Castiglione Morelli. 1991. Solution conformation of salmon calcitonin in sodium dodecyl sulfate micelles as determined by two-dimensional NMR and distance geometry calculations. *Biochemistry.* 30:10444–10450.

Sahl, H. G., M. Kordel, and R. Benz. 1987. Voltage-dependent depolarization of bacterial membranes and artificial lipid bilayers by the peptide antibiotic nisin. *Arch. Microbiol.* 149:120–124.

Schmidt, M. C., B. Rothen-Rutishauser, B. Rist, A. Beck-Sickinger, H. Wunderli-Allenspach, W. Rubas, W. Sadee, and H. P. Merkle. 1998. Translocation of human calcitonin in respiratory nasal epithelium is associated with self-assembly in lipid membrane. *Biochemistry.* 47: 16582–16590.

Segre, G. V., and S. R. Goldring. 1993. Receptors for secretin, calcitonin, parathyroid hormone (PTH/PTH related peptide), vasoactive intestinal peptide, glucagon-like peptide 1, growth hormone-releasing hormone, and glucagon belong to a newly discovered G-protein-linked receptor family. *Trends Endocrinol. Metab.* 4:309–314.

Sexton, P. M., D. M. Findlay, and T. J. Martin. 1999. Calcitonin. *Curr. Med. Chem.* 6:1067–1093.

Siligardi, G., B. Samori, S. Melandri, M. Visconti, and A. F. Drake. 1994. Correlations between biological activities and conformational properties for human, salmon, eel, porcine calcitonins and Elcatonin elucidated by CD spectroscopy. *Eur. J. Biochem.* 221:1117–1125.

Torres-Lugo, M., and N. A. Peppas. 2000. Transmucosal delivery systems for calcitonin: a review. *Biomaterials.* 21:1191–1196.

Tosteson, M. T., O. Alvarez, W. Hubbell, R. M. Bieganski, C. Attenbach, L. H. Caporales, J. J. Levy, R. F. Nutt, M. Rosenblatt, and D. C. Tosteson. 1990. Primary structure of peptides and ion channels. Role of amino acid side chains in voltage gating of melittin channels. *Biophys. J.* 58:1367–1375.

Wallach, S., G. Rousseau, L. Martin, and M. Azria. 1999. Effects of calcitonin on animal and in vitro models of skeletal metabolism. *Bone.* 25:509–516.

Williams, R. W., R. Starman, K. M. Taylor, K. Gable, T. Beeler, and M. Zasloff. 1990. Raman spectroscopy of synthetic antimicrobial frog peptides magainin 2a and PLGa. *Biochemistry.* 29:4490–4496.